analytical chemistry

Article

pubs.acs.org/ac

Counting Small RNA in Pathogenic Bacteria

Douglas P. Shepherd,[†,‡] Nan Li,[§] Sofiya N. Micheva-Viteva,[§] Brian Munsky,[‡,§,∥] Elizabeth Hong-Geller,[§] and James H. Werner[†,*]

[†]Center for Integrated Nanotechnologies, Los Alamos National Laboratory, Los Alamos, New Mexico 87545, United States

[‡]Center for Nonlinear Studies, Los Alamos National Laboratory, Los Alamos, New Mexico 87545, United States

[§]Bioscience Division, Los Alamos National Laboratory, Los Alamos, New Mexico 87545, United States

[∥]Information Sciences Group, Los Alamos National Laboratory, Los Alamos, New Mexico 87545, United States

Supporting Information

ABSTRACT: Here, we present a modification to single-molecule fluorescence in situ hybridization that enables quantitative detection and analysis of small RNA (sRNA) expressed in bacteria. We show that short (~200 nucleotide) nucleic acid targets can be detected when the background of unbound singly dye-labeled DNA oligomers is reduced through hybridization with a set of complementary DNA oligomers labeled with a fluorescence quencher. By neutralizing the fluorescence from unbound probes, we were able to significantly reduce the number of false positives, allowing for accurate quantification of sRNA levels. Exploiting an automated, mutli-color wide-field microscope and data analysis package, we analyzed the statistics of sRNA expression in thousands of individual bacteria. We found that only a small fraction of either *Yersinia pseudotuberculosis* or *Yersinia pestis* bacteria express the small RNAs YSR35 or YSP8, with the copy number typically between 0 and 10 transcripts. The numbers of these RNA are both increased (by a factor of 2.5× for YSR35 and 3.5× for YSP8) upon a temperature shift from 25 to 37 °C, suggesting they play a role in pathogenesis. The copy number distribution of sRNAs from bacteria-to-bacteria are well-fit with a bursting model of gene transcription. The ability to directly quantify expression level changes of sRNA in single cells as a function of external stimuli provides key information on the role of sRNA in cellular regulatory networks.

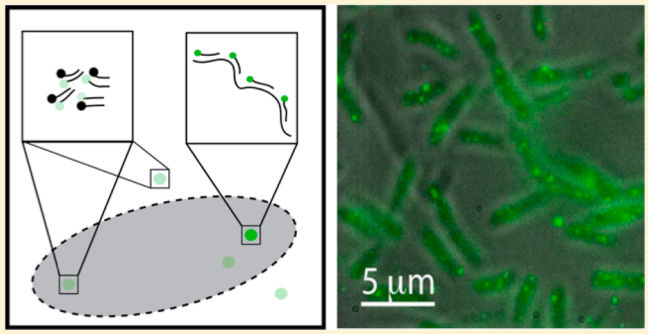

Single cell measurements of gene expression have provided key insights into how messenger RNA (mRNA) are produced,[1] the regulatory role of long noncoding RNA,[2] and determination of cell fate by spatial patterning. One key method used to obtain single cell expression data is single-molecule fluorescence hybridization (smFISH), a technique first introduced for RNA localization by the Singer group,[3] with Raj and Tyagi introducing refinements in probe design and demonstrating how the method could be used to explore gene regulatory networks.[4]

In the smFISH technique, individual cells are permeabilized, fixed by chemical cross-linking, and labeled with ~40 fluorescently labeled DNA oligos that target a specific mRNA. Each fluorescently labeled DNA oligo is complementary to a different short sequence in the mRNA, such that each mRNA transcript can be visualized as a bright spot in an epi-fluorescence microscope. These spots are easily distinguished from the background of single isolated probes. Unlike RT-PCR or DNA hybridization arrays, which measure the response of large cell populations, smFISH works directly on individual cells, such that cell-to-cell heterogeneity and subpopulations are directly observed. Moreover, smFISH is highly quantitative, as the number of mRNA transcripts is directly measured (counted) at the single molecule level without any enzymatic amplification steps.

While many groups have successfully applied smFISH to study mRNA expression in prokaryotes and eukaryotes,[5−8] little progress has been made on quantitative studies of small RNAs (sRNAs) at the single-transcript/single-cell level. This is primarily due to the limited number of fluorescent probes that can be hybridized simultaneously to a single sRNA target. With the use of the smFISH probe design rules of Raj et al., fluorescent probes for smFISH are ~20 nt long with a guanine-cytosine (G-C) content near ~50%, and individual probe sequences are selected to avoid repetitive and problem sequences.[4] These design rules are typically easy to satisfy in mRNA, as the sequences are well-known and thousands of nucleotides in length. This is not the case with sRNA, which is substantially shorter (tens to hundreds of nucleotides) compared to mRNA. In addition, the reported sequences in the literature typically vary between techniques used. For example, Koo et al. report variation in sequences as determined

Received: December 29, 2012
Accepted: April 11, 2013
Published: April 11, 2013

   dx.doi.org/10.1021/ac303792p | *Anal. Chem.* 2013, 85, 4938−4943

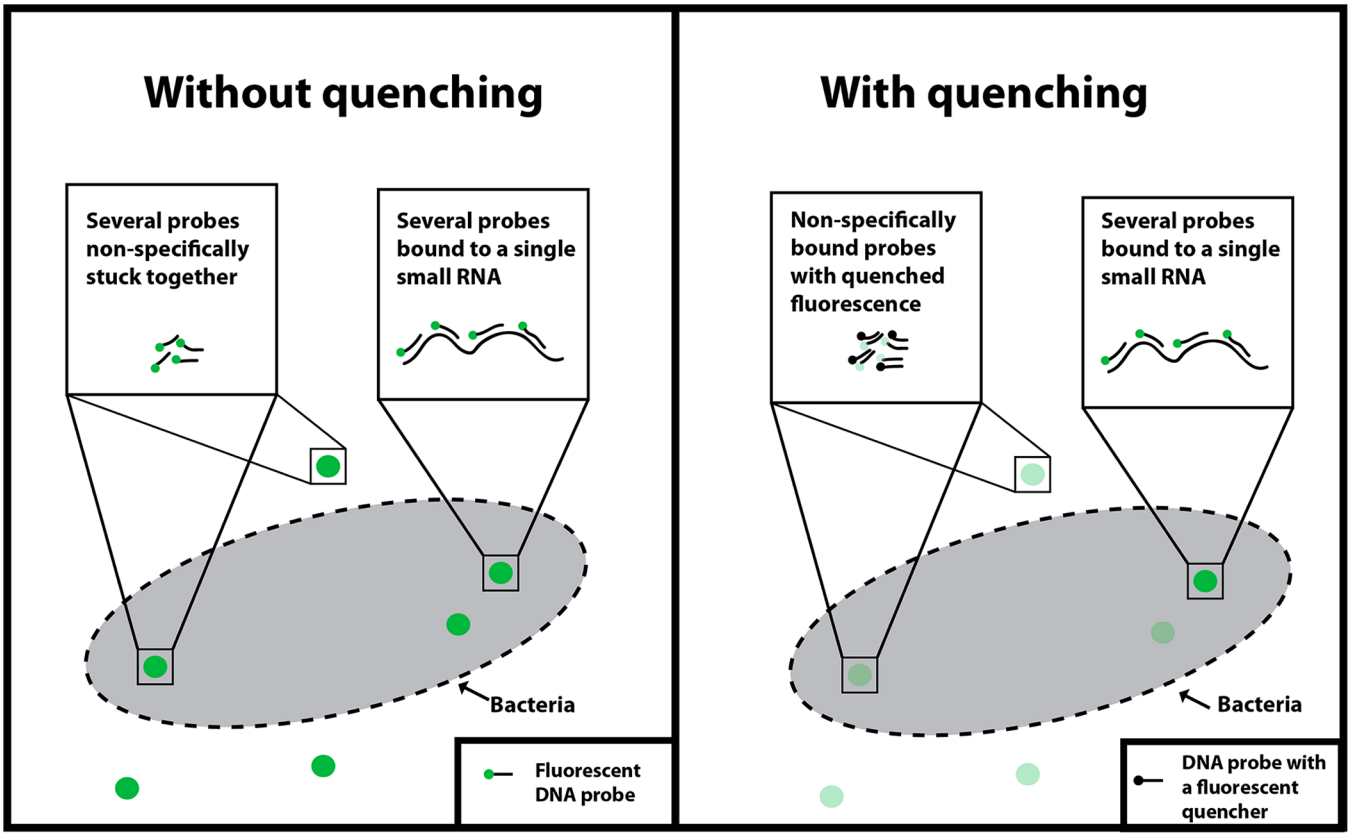

Figure 1. Illustration of specifically bound and nonspecifically bound fluorescent probes on sample surface. Bacteria are represented by gray ellipses, smFISH probes by green circles with short black lines, quencher probes by black circles with short black lines, and larger green circles are used to denote the fluorescence coming from a number of probes that reside inside a diffraction-limited volume element. The fluorescence from quenched probes is shown as a more translucent shade of green. Without (A) quenchers, unbound probes in close proximity are seen as a single spot that is bright enough to be a true sRNA target, which leads to false positive detections. By hybridizing quenchers to (B) unbound probes, it is possible to reduce the false positive rate and aid in quantitative detection of sRNA targets.

by high-throughput sequencing and rapid amplification of cDNA ends (RACE) for all sRNAs they identified in *Yersinia pseudotuberculosis*.[9] To hybridize a smaller number (e.g., 5−10) of probes to a sRNA target, the design rules of ∼50% G-C content, large separation between individual probes, and avoiding repetitive sequences must be substantially relaxed, which leads to higher nonspecific binding and lower hybridization efficiencies. In particular, for both sRNA targets investigated in this work, the total number of probes bound to single transcripts varied greatly, a result we attribute to this relaxed probe design. To offset these lower hybridization efficiencies, we found it necessary to introduce orders of magnitude more smFISH probes into each sRNA sample than is required for mRNA labeling and detection. While this increase in probe concentration increases the number of probes hybridized to each sRNA target, it also introduces a higher false positive rate due to unbound probes and nonspecific binding of probes. Figure 1a is a schematic illustration of this situation, where the higher concentration of probes leads to aggregates of multiple nonspecifically bound DNA probes, skewing counts of individual sRNA in a single bacterium and the statistics of sRNA expression in a population of cells. As expression levels of sRNA can vary from zero to a large number of transcripts per bacterium, accurate counting of single transcripts is key to the quantitative investigation of regulatory networks.[10]

Here, we present a technique to reduce the occurrence of false positive detection of selected sRNA targets and improve quantitative measurements of changes of sRNA expression in an imaging format. This method reduces background and false positive detection by using fluorescence quenching to neutralize unbound probes within bacterial cells. The technique is an extension of a similar procedure applied by Nolan et al. to detect mRNA in solution.[11] Figure 1b illustrates how this method reduces background and false positive detection of sRNA. The method relies upon the likelihood that unbound fluorescent probes and nonspecifically bound probes are sufficiently exposed to hybridize with complementary oligomers. We note that this method can not quench the fluorescence from probes that are well-hybridized with another nucleic acid but does lower the background from unbound probes or probes that may only be partially hybridized to a target. Combined with a choice in fluorescent hybridization probes that minimizes overlap with the rest of the transcriptome, this technique will still be applicable to more complicated transcriptomes (such as mammalian cells). In this method, the fluorescence neutralizing oligomers are conjugated with a fluorescence quencher that absorbs the energy from the excited state of the fluorescent dye through fluorescent resonant energy transfer (FRET) and then dissipates this energy through nonemissive pathways.[12] By quenching the unbound probes, the number of false fluorescent spots is reduced, which improves the accuracy of the count statistics and significantly reduces the image processing time.

dx.doi.org/10.1021/ac303792p | *Anal. Chem.* 2013, 85, 4938−4943

EXPERIMENTAL SECTION

Identification of Target sRNA. We selected the Yersinia-specific sRNA-35 (YSR35) for single molecule analysis, based on its relatively long sequence length (>200 nt) for a sRNA and its time-dependent upregulation upon a temperature shift from 25 to 37 °C, suggesting that YSR35 may play a role in infection of the human host.[9] We have also performed ultra high-throughput sequencing of the *Y. pestis* transcriptome to identify novel Yersinia sRNAs involved in pathogenesis. (Manuscript in preparation, Hu, Stubben, and Chain). From this sequencing work, we selected a novel sRNA, termed sRNA-8 (YSP8), for single molecule analysis in *Y. pestis*.

smFISH Probe Sets. Probe sets were purchased from Biosearch Technologies, utilizing a probe designer that maximizes G-C content of individual probes while ensuring minimal nonspecific binding. For *Y. pestis* sRNA-8 (YSP8), Cal Fluor 590 dye was used as the fluorescent reporter. For *Y. pseudotuberculosis* sRNA-35 (YSR35) experiments, two separate probe sets using Quasar 560 and Cal Fluor 590 dyes as fluorescent reporters were utilized. Probe sets were diluted to 100 μM concentrations in nuclease-free water and aliquoted into 5 μL batches for subsequent experiments. Complementary oligos to each probe in a given probe set were designed with Black Hole Quencher 2 at the 5′ end (Biosearch Technologies). Individual probes were diluted to 1 μM concentrations in nuclease-free water and aliquoted into 5 μL batches for subsequent experiments. The sequences of all probes and complementary oligos can be found in the Supporting Information.

Hybridization of the probes to target sRNA was performed in a hybridization buffer that consisted of 1 g dextran sulfate, 10 mg *Escherichia coli* tRNA, 100 μL of 200 mM vandayl ribonucleoside complex (NEB), 40 μL of 50 mg/mL bovine serum albumin (BSA) (RNase free) (Ambion), 1 mL 20× saline-sodium citrate (SSC) (nuclease free, Ambion), 5 mL formamide (deionized, Ambion), with a final solution volume of 10 mL. We arrived at the 50% formamide concentration by performing a dilution series of 10−70% formamide in 10% increments, with 50% yielding the best signal-to-noise at these high probe concentrations. Sample washing was performed in a buffer consisting of 5 mL of 20× SSC (RNase free, Ambion), 25 mL formamide (deionized, Ambion), and 20 mL nuclease-free water.

***Y. pestis* and *Y. pseudotuberculosis* Culturing and Fixation.** *Y. pseudotubuculosis* (ATCC 4284) or *Y. pestis* (CO92, Δ*pgm*) was grown overnight in brain heart infusion (BHI) medium at 25 °C. An aliquot of bacterial culture was diluted in BHI medium supplemented with 2.5 mM $CaCl_2$ to an OD_{600} of 0.1 and allowed to grow at 25 or 37 °C for an additional 2−3 h. Bacterial pellets were then collected by centrifugation at 6000*g* for 5 min and fixed in 3.7% formaldehyde for 30 min at room temperature, followed by overnight permeabilization in 70% ethanol at 4 °C.

smFISH Hybridization. Fixed and permeabilized bacterial samples were centrifuged in an Eppendorf 5418 centrifuge at 5000 rpm for 10 min. The ethanol was aspirated off the bacteria, and 300 μL of wash buffer was added to each tube. After 5 min, the bacteria were centrifuged again, the wash buffer aspirated, and 300 μL of hybridization buffer was added. For hybridization, a probe set was diluted in hybridization buffer at a 1:100 ratio. The samples were incubated overnight at 30 °C in the dark. The bacteria were then centrifuged and washed twice using 30 min incubations at 30 °C with 300 μL of wash buffer. The cell samples were finally resuspended in 300 μL of 2× SSC buffer.

Background Reduction by Complementary Quenchers. Because fluorescent hybridization probes are pooled together in the probe sets obtained from Biosearch Technologies, we only have a rough estimate for the concentration of individual probes within our samples. We found that a 10-fold greater abundance of quenched probes was capable of nearly completely quenching the fluorescence from the smFISH fluorescent probes in solution. Thus, for the imaging experiments, we diluted 25−100 μL of bacteria that have been fluorescently labeled with the smFISH probes into 200 μL of the quencher solution (with a quencher concentration of 10× that of the smFISH probe concentration).

Bulk Fluorimetry Measurements. The fluorescence of a probe set with or without quenchers in hybridization buffer and hybridization buffer alone was measured using a Varian Cary Eclipse fluorescence spectrophotometer. The path length of the cuvette is 1 cm (16.100F-Q-10/z15, Starna Cells).

Multiplexed Two-Dimensional Imaging. We adapted our arc lamp-based multiplexed three-dimensional (3D) microscope[8] to perform laser-based multiplexed two-dimensional imaging. The imaging system is constructed on an Olympus IX71 inverted microscope with a motorized six-filter cube turret. Excitation is provided by a 532 or a 561 nm solid state laser (Crystalaser) and filtered by a Semrock dichroic (Di02-R532 for 532 nm excitation and Di01-R405/488/561/635 for 561 nm excitation). The 532 and 561 nm lasers provide excitation for the Quasar 570 and Cal Fluor 590 dyes, respectively. One of the six filter cube positions is left blank for white light imaging. The objective is an Olympus APO N 60×/1.49 TIRF oil objective and is mounted onto a Physik Instrumente Z-piezo (PI 721.20) to allow for Z sectioning through the sample. A Thor Laboratories MAX200 positioning stage is mounted to the microscope and a custom sample stage allows for secure mounting of no. 1 coverslips with 10−20 μL of sample sandwiched by another no. 1 coverslip. A Princeton Instruments ProEM electron-multiplying CCD (EMCCD) camera is used for image acquisition.

The positioning stage, EMCCD, and Z-piezo are all interfaced to LabVIEW through USB, GIG-E, and a digital-to-analog converter board, respectively. Custom LabVIEW control software enabled automated collection of variable size Z-stacks at multiple areas per sample slide. The software initially collects a white light Z-stack and then excitation/emission by rotating the filter turret to the cube containing the laser dichroic and stepping through the Z-plane by moving the piezo. A 10 μm Z-stack is used to compensate for microscope drift over the time course of the experiment. Depending upon the concentration of cells, we imaged between 50 and 400 areas per slide, with a step size in X and Y of 100 μm. The number of bacteria analyzed varied from thousands to tens of thousands depending on the number of image areas acquired. A typical imaging run takes 6−8 h, followed by 2−3 days of data processing.

Data Processing. The data processing is performed using custom Matlab code (available upon request) that follows a general outline of image filtering, spot identification, two-dimensional (2D) Gaussian fitting, spatial assignment of individual bacteria, and finally spatial assignment of fluorescent spots to bacteria. Each of these tasks is completed by a subroutine, which we describe briefly below.

dx.doi.org/10.1021/ac303792p | *Anal. Chem.* 2013, 85, 4938−4943

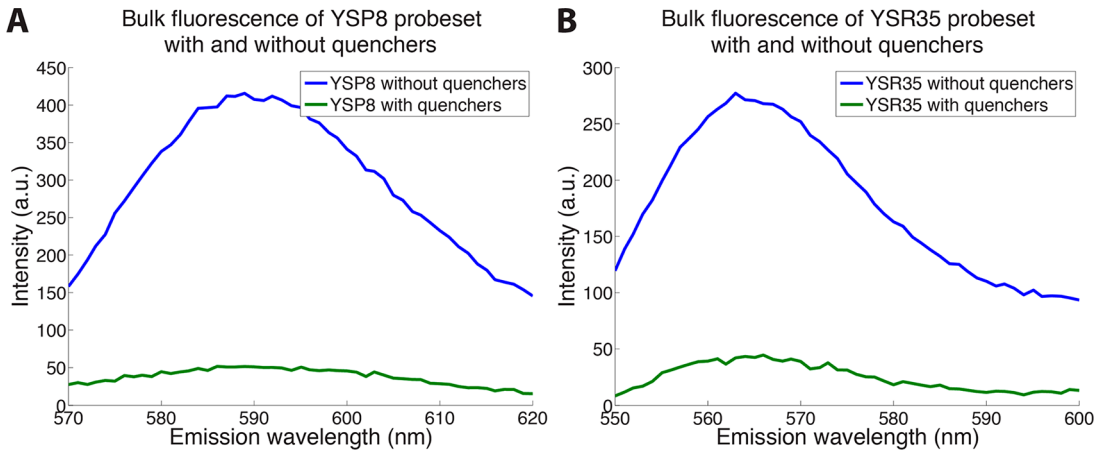

Figure 2. Bulk fluorescence measurements of (A) YSP8 probes with and without quenchers and (B) YSR35 probes with and without quenchers. For each probe set, a greater than eight-fold reduction in peak fluorescence intensity occurs upon addition of the complementary quencher set. The background of hybridization buffer is subtracted from all scans, and the concentration of probes is kept constant for all experiments.

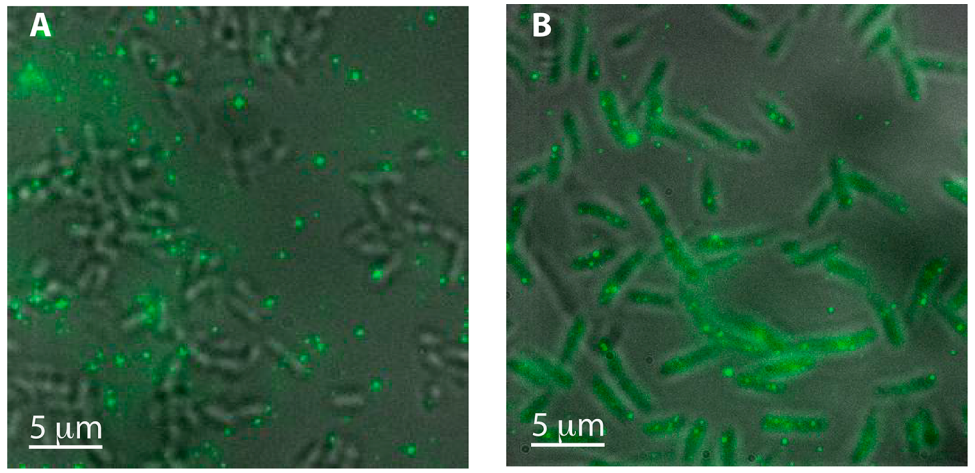

Figure 3. False color images of *Y. pseudotuberculosis* after smFISH hybridization of (A) YSR35 probe set and (B) YSR35 probe set and complementary quenchers. The fluorescence intensity in each image is normalized and colored green for visualization. Without quenchers, the majority of measured fluorescence is outside of the bacteria, compounding our ability to localize individual YSR35 sRNA. With quenchers, the majority of fluorescence is localized within bacteria and nonspecifically bound probes are easily differentiated from labeled YSR35 transcripts.

First, we find the image plane(s) containing the sample surface by counting the number of fluorescent spots in each image plane of the Z-stack and selecting the six image planes around the Z-slice that contained the most spots. We then discard the other image planes in the Z-stack before we continue with the rest of the data analysis.

Second, we find all bacteria that are fixed to the coverslip in the sample. A 3D Laplacian of a Gaussian (LoG) filter is applied to enhance bacterial-sized objects within the Z-stack. After the LoG filter is applied, we compute the standard deviation of each pixel over all images in the z-stack to normalize the resulting image. A watershed gradient algorithm[13] is applied to the 2D image to identify all objects that are potentially bacteria. Those objects that are too large to be bacteria or move throughout the Z-stack are discarded. Finally, we create an (X,Y) pixel list for all identified bacteria in the image.

Third, we find all potential fluorescent-labeled sRNA targets in the sample. We form a maximum intensity projection (MIP) for each smFISH z-stack. This MIP image is convolved with a 2D Laplacian of a Gaussian (LoG) filter to enhance diffraction limited fluorescence spots within the Z-stack. After the LoG filter is applied, the image is normalized and a low-pass filter is applied to remove any matrix elements with values less than 0.2. A 2D 9-membered matrix (3×3) of zeros and ones is then used in conjunction with a flood-fill algorithm[13] to determine objects that are connected in two-dimensions. Every object that meets the connected criteria is given a unique identifier, and its centroid is recorded. We then implement a fast 2D Gaussian fitting routine to obtain the amplitude, width, noise, and (X,Y) position of a 2D Gaussian fit to every identified object.[14] Those objects that cannot be fit are removed from the object list, as well as those with Gaussian amplitudes corresponding to single fluorescent dye molecules (approximately 1500 for our optical setup at 100× EMCCD gain).

Finally, we assign fluorescent spots to bacteria by comparing the (X,Y) position from the Gaussian fitting routine to the (X,Y) pixels of each bacteria. If a match is found, the assignment is made to the corresponding bacteria and the next fluorescent spot evaluated. If no match is found, the spot is discarded as background.

dx.doi.org/10.1021/ac303792p | *Anal. Chem.* 2013, 85, 4938−4943

RESULTS

We first verified that combining the fluorescent probe and quenching probes at a 1:10 ratio per individual probe can reduce the bulk fluorescence signal. The fluorescence from the smFISH probes was efficiently quenched in solution by hybridization with the corresponding quenching probe sets for both YSP8 (Figure 2A) and YSR35 (Figure 2B).

We next utilized the fluorescent quenchers to reduce the background in smFISH imaging experiments. In *Y. pseudotuberculosis* cells labeled with YSR35 probes without quenchers (Figure 3A), unbound probes on the surface and nonspecifically bound probes inside bacteria contribute to the nonspecific background signal. While this fluorescent background is present in smFISH-based detection of mRNA, it does not impede the accurate quantification of mRNA because there are an order of magnitude more probes bound to the longer mRNA target. Given the smaller size and more relaxed design constraints of the YSR35 probes, individual fluorescently labeled sRNA in Figure 3a are difficult to discern due to large extracellular aggregates that dominate the background. To accurately quantify sRNA expression greater than 10000 bacteria per experimental condition, user intervention is normally required to decide the appropriate background and curate spots for false positives. Upon quenching, the remaining fluorescent spots are diffraction-limited points within a single bacteria, and we can automatically determine the background and discard false positives and unquenched individual probes (Figure 3b).

After achieving this marked reduction in false positives, we then investigated the change in expression levels of both YSP8 and YSR35 due to temperature change from 25 to 37 °C, which corresponds to a shift from *Y. pestis* infection conditions of the flea host to a human host during infection. Figure 4A shows the

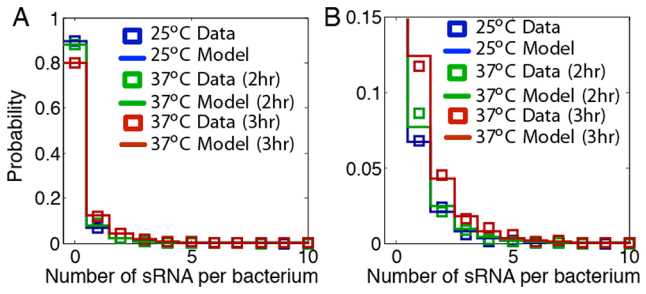

Figure 4. Expression level change of YSP8 sRNA in *Y. pestis* due to a temperature shift from 25 to 37 °C after two and three hours. (A) The number of YSP8 sRNA in all bacteria and model fits. (B) A blow up showing only those bacteria that contain one or more copies of YSP8 sRNA. The majority of bacteria are sRNA-, producing no YSP8 sRNA at 25 or 37 °C. The YSP8 expression distribution has a long geometric tail, consistent with a bursting gene expression model. The overall fold change from 25 to 37 °C at three hours is a 4× up-regulation, confirmed by RT-PCR.

probability (derived from approximately 30000 bacteria) that a given *Y. pestis* CO92 bacterial cell will contain a particular number of YSP8 sRNAs at 25 °C (blue squares), two hours at 37 °C (green squares), and three hours at 37 °C (red squares). The majority of bacteria do not appear to express YSP8 sRNA. A small fraction, ∼20% of the population, produces more than one YSP8 transcript (Figure 4B), which shows sRNA distributions only for bacteria that contain 1 or more copies of YSP8. After 3 h at 37 °C, *Y. pestis* upregulates YSP8 by ∼3.5×, suggesting that YSP8 may be utilized during human infection. Our smFISH analysis was further confirmed by RT-PCR experiments, in which we see an approximately four-fold increase in YSR8 expression in *Y. pestis* upon a temperature shift to 37 °C.

A similar analysis for *Y. pseudotuberculosis* was used to determine the probability (derived from approximately 20000 bacteria) that a given cell will contain a specific number of YSR35 sRNAs at 25 °C (blue squares) and after two hours at 37 °C (red squares) (Figure 5A). Again, we find that the

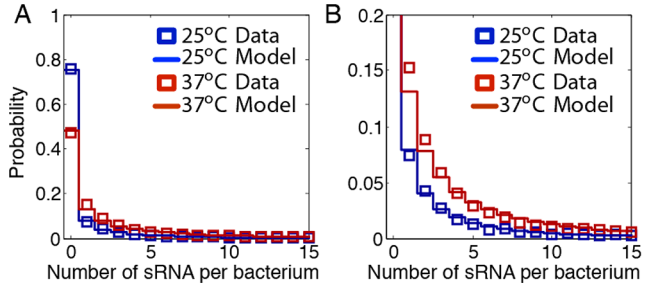

Figure 5. Expression level change of YSR35 sRNA in *Y. pseudotuberculosis* due to a temperature shift from 25 to 37 °C at two hours. (A) The number of YSR35 sRNA in all bacteria and model fits. (B) A blow up showing only those bacteria that contain one or more copies of YSR35 sRNA. The majority of bacteria are sRNA-, producing no YSR35 sRNA at 25 or 37 °C. The long geometric tail of the YSR35 expression at both temperatures is consistent with temperature modulation of burst frequency. The overall fold change from 25 to 37 °C at two hours is a 2× up-regulation, confirmed by RT-PCR.

majority of bacteria do not express YSR35. However, upon a temperature shift from 25 to 37 °C, the number of bacteria expressing one or more copies of YSR35 increases by a factor of approximately 2.5 (Figure 5B), a finding that matches RT-PCR measurements averaged over a bacterial population.[9]

The rapid decay in sRNA copy number per bacteria shown in Figures 4 and 5 are indicative of a "bursting" mechanism of transcription, where the sRNA are produced for a discrete period of time at stochastic intervals.[15] We postulated that up-regulation of YSR35 and YSP8 upon temperature shift increases either the burst amplitude (i.e., the average number of sRNA produced per burst) or decreases the waiting time between bursts (i.e., increases burst frequency). These model mechanisms were recently reviewed,[16] which discussed how either mechanism can change the bulk RNA expression but exhibit different effects on the RNA variance and distribution shape. Following our approach to identify stochastic models for protein[17,18] and mRNA[19] distributions, we used finite state projection analyses[20] to fit each mechanism to the full YSR35 and YSP8 sRNA distributions. We found that frequency modulation (i.e., changing k_{ON} of the gene transcription) is sufficient to capture the changes in sRNA distributions for both sRNA (Figures 4 and 5). Conversely, we found that amplitude modulation (i.e., changing k_{OFF} of the gene transcription) did a poorer job to capture the sRNA statistics at both temperatures (see Figures S1 and S2 of the Supporting Information).

An interesting finding of this work is the relatively low sRNA copy number we find in both bacterial populations, raising the question of how many sRNAs are required to enact regulatory control over mRNA and protein populations? We note that approximately 20% of the proteins in *E. coli* are present at one copy number or less, suggesting low copy numbers may be

dx.doi.org/10.1021/ac303792p | *Anal. Chem.* 2013, 85, 4938−4943

ubiquitous in bacteria.[5] To further investigate the regulatory role of these sRNA, we are currently applying the methodology presented in this work to simultaneously measure sRNA in addition to measuring single cell mRNA distributions for mRNAs that are potential regulatory targets of YSR35 and YSP8.

CONCLUSION

We have demonstrated quantitative measurement of expression changes of two distinct small RNAs in *Y. pestis* and *Y. pseudotuberculosis*. By quenching the fluorescence from unbound probes and compensating for smFISH probe design deficiencies due to the shorter lengths of typical sRNAs (<500 nucleotides), we have reduced the number of false positives present in these single cell measurements. Using this method, we find that only a small fraction of bacteria in a large population (>10000 bacteria) express YSR35 or YSP8, with the copy number typically between 0 and 10 transcripts. Due to these low copy numbers, reducing the number of false positives becomes even more critical to correctly determine the expression statistics for these sRNAs. Investigating the underlying system dynamics and determining how large of an effect these sRNAs have on the expression of mRNA targets represent future areas of research that are currently being pursued.

ASSOCIATED CONTENT

Supporting Information

A list of DNA sequences used in this work for both the sRNA probes and the complementary quenchers, along with alternate model fits, are provided in the Supporting Information. This material is available free of charge via the Internet at http://pubs.acs.org.

AUTHOR INFORMATION

Corresponding Author

*E-mail: jwerner@lanl.gov.

Author Contributions

The manuscript was written through contributions of all authors. All authors have given approval to the final version of the manuscript.

Funding

This work was supported through Los Alamos National Laboratory Directed Research and Development (LDRD) and was in part performed at the Center for Integrated Nanotechnologies, a U.S. Department of Energy, Office of Basic Energy Sciences user facility at Los Alamos National Laboratory (Contract DE-AC52−06NA25396).

Notes

The authors declare no competing financial interest.

ACKNOWLEDGMENTS

The authors acknowledge B. Hu, C. Stubben, and P. Chain for their work on sRNA discovery in *Yersinia pestis*. The authors also thank Yulin Shou for technical assistance with *Y. pestis* samples.

ABBREVIATIONS

sRNA, small ribonucleic acid; mRNA, messenger ribonucleic acid; smFISH, single-molecule fluorescence in situ hybridization; LoG, Laplacian of a Gaussian; YSP, *Yersinia pestis*; YSR, *Yersinia* Specific RNA; BSA, bovine serum albumin; SSC, saline-sodium citrate

REFERENCES

(1) Lionnet, T.; Singer, R. H. *EMBO Rep.* **2012**, *13* (4), 313−321.
(2) van Werven, F. J.; Neuert, G.; Hendrick, N.; Lardenois, A.; Buratowski, S.; van Oudenaarden, A.; Primig, M.; Amon, A. *Cell* **2012**, *150*, 1170−1181.
(3) Femino, A. M.; Fay, F. S.; Fogarty, K.; Singer, R. H. *Science* **1998**, *280* (5363), 585−590.
(4) Raj, A.; van den Bogaard, P.; Rifkin, S. A.; van Oudenaarden, A.; Tyagi, S. *Nat. Methods* **2008**, *5* (10), 877−879.
(5) Taniguchi, Y.; Choi, P. J.; Li, G. W.; Chen, H.; Babu, M.; Hearn, J.; Emili, A.; Xie, X. S. *Science* **2010**, *329* (5991), 533−538.
(6) Raj, A.; Peskin, C. S.; Tranchina, D.; Vargas, D. Y.; Tyagi, S. *PLoS Biol.* **2006**, *4* (10), e309.
(7) Suter, D. M.; Molina, N.; Gatfield, D.; Schneider, K.; Schibler, U.; Naef, F. *Science* **2011**, *332* (6028), 472−474.
(8) Shepherd, D. P.; Li, N.; Hong-Geller, E.; Munsky, B.; Werner, J. H. *Proc. SPIE* **2012**, 822808−822808.
(9) Koo, J. T.; Alleyne, T. M.; Schiano, C. A.; Jafari, N.; Lathem, W. W. *Proc. Natl. Acad. Sci. U.S.A.* **2011**, *108* (37), E709−E717.
(10) Waters, L. S.; Storz, G. *Cell* **2009**, *136* (4), 615.
(11) Nolan, R. L.; Cai, H.; Nolan, J. P.; Goodwin, P. M. *Anal. Chem.* **2003**, *75* (22), 6236−6243.
(12) Morrison, L. E. *J. Fluoresc.* **1999**, *9* (3), 187−196.
(13) Sedgewick, R. *Algorithms in C, Parts 1-4: Fundamentals, Data Structures, Sorting, Searching*; 3rd edition; Addison-Wesley Publishing Co.: White Plains, NY, 1997.
(14) Anthony, S. M.; Granick, S. *Langmuir* **2009**, *25* (14), 8152−8160.
(15) Elowitz, M. B.; Levine, A. J.; Siggia, E. D.; Swain, P. S. *Sci. Signaling* **2002**, *297* (5584), 1183.
(16) Munsky, B.; Neuert, G.; van Oudenaarden, A. *Science* **2012**, *336* (6078), 183−187.
(17) Munsky, B.; Trinh, B.; Khammash, M. *Mol. Syst. Biol.* **2009**, *5* (1).
(18) Lou, C.; Stanton, B.; Chen, Y. J.; Munsky, B.; Voigt, C. A. *Nat. Biotechnol.* **2012**, *30* (11), 1137−1142.
(19) Neuert, G.; Munsky, B.; Tan, R.-Z.; Teytelman, L.; Khammash, M.; Oudenaarden, A. v. *Science* **2013**, *339*, 584−587.
(20) Munsky, B.; Khammash, M. *J. Chem. Phys.* **2006**, *124*, 044104.